

Supplementary Materials for
A Facile, General, and Modular Synthetic Approach to
Biomass-based Diols

*Le Jiang,^a Li Wang,^a Qiang Yan,^b Haojun Fan^a and Jun Xiang^{*a}*

^aCollege of Biomass Science and Engineering, Sichuan University, Chengdu
610065, China

^bState Key Laboratory of Molecular Engineering of Polymers, Department of
Macromolecular Science, Fudan University, Shanghai 200433, P.R. China

Corresponding Author: junxiang@scu.edu.cn

1. Materials. 1,6-Diisocyanohexane (DICH) (>99%) was obtained from Guang Ao Co., Ltd (Hubei, China). Biomass-based acetic acid (C2, 99%), butyric acid (C4, 99%), caproic acid (C6, 99%), octanoic acid (C8, 99%), capric acid (C10, 99%), 10-undecenal (UA, >97%), 2-hydroxy-2-methylpropiophenone (HM, >98%), 1,3-butanediol (BD, 99%) were purchased from Adamas-beta Regent Co., Ltd (Shanghai, China). Petroleum ether (60–90 °C, >99%), ethyl acetate (>99%), *N, N*-dimethylformamide (DMF) (>99%), organic bismuth catalyst, and triethylamine (TEA) were supplied by Chron Chemicals Co., Ltd (Chengdu, China). 2-Mercaptoethanol (MO) was provided by TCL Development Co., Ltd (Shanghai, China). Isophorone diisocyanate (IPDI) was obtained from Dymatic Post Polymer Material Co. (Lishui, China). 2,2-Bis(hydroxymethyl) propionic acid (DMPA) was supplied by Sigma-Aldrich (Shanghai, China).

2. Pathways for the Production of the Starting Materials from Biomass Resource.

2.1 10-undecenal (UA). In the previous work, Meier et al. highlighted the renewable nature of 10-undecenal (UA) and elucidated the methods by which it can be derived from the castor oil plant.^[1] Briefly, UA can be prepared through the reduction of the pyrolysis product of ricinoleic acid, known as 10-undecenoic acid. As ricinoleic acid is sourced from the castor plant,^[2] UA can be effectively produced from biomass resources.

2.2 1,6-diisocyanohexane (DICH). Previous research has demonstrated that the synthesis of 1,6-diisocyanohexane (DICH) can be accomplished through either a one- or two-step procedure, with 1,6-diaminohexane serving as the primary raw material (the highest yield: 92%).^[3, 4] Additionally, numerous reviews have comprehensively outlined the metabolic pathways associated with 1,6-diaminohexane.^[5-7] Consequently, it is feasible to produce DICH from biomass resources.

2.3 Acetic acid (C2). According to the previous study, acetic acid (C2) can be derived from the pyrolysis oil of lignocellulosic biomass. For detailed information, please refer to the reference published by Franco Berruti and co-workers.^[8]

2.4 Butyric acid (C4). In the publication by Salvachúa et al., a comprehensive, integrated process for the production of butyric acid (C4) from lignocellulosic sugars is presented.^[9] The study demonstrates that the selling price of butyric acid obtained through this process is considerably lower compared to petroleum-derived sources. Consequently, it can be concluded that C4 can be effectively produced from biomass resources.

2.5 Caproic acid (C6). In the study conducted by Kroeze et al., it is demonstrated that caproic acid (C6) can be synthesized from mixed organic waste.^[10] For further details, please refer to the relevant reference provided in their work.

2.6 Octanoic acid (C8). In the work conducted by Hwang et al., the authors claimed that octanoic acid can be synthesized utilizing a biological approach.^[11] This biomass-derived compound finds application in various industries such as dye production, perfume formulation, pesticide development, and disinfectant manufacturing due to its notable antimicrobial properties.

2.7 Capric acid (C10). In their publication, Gonzalez and Kim presented a remarkable engineered cell factory capable of producing capric acid (C10) as a predominant product using glycerol as an abundant and renewable feedstock. For further details, please refer to that reference.^[12]

2.8 2-Mercaptoethanol (MO). 2-Mercaptoethanol (MO) can be generated through the reaction of ethylene oxide with hydrogen sulfide. In this process, ethylene oxide can be obtained from bio-ethanol derived from sugar cane or corn.^[13] Thus, MO can be partially obtained from renewable biomass resources.

Comments on the complexity of the formation pathways and the overall yield of these starting materials. *First, we would like to emphasize that, although the transformation pathways may appear somewhat complex in references given in the Supporting Information, all of the starting materials used in this study are commercially available. Furthermore, we would like to highlight that against the backdrop of increasing and alarming signals of climate change, there is a growing interest among individuals and industries to reduce their environmental footprints. The demand for bio-based chemicals has been experiencing strong growth in recent years and is expected to continue in the coming years. With continuous technological advancements and the implementation of relevant policies (such as the ‘double carbon’ policy in my country), the prices of biomass-derived chemicals are projected to further decrease.*

3. Characterizations. The structural analysis of biomass-based dienes and diols was carried out using a Bruker AV III HD-400 MHz spectrometer (Bruker, Germany). The molecular weights of dienes and diols were determined using a TSQ Quantum Ultra AM mass spectrometer (HermoFisherScienti, USA). The hydroxyl values were determined according to GB/T 12008.3-2009. The water absorption capacity of BWPU films was determined by the following experimental procedures. The sample was trimmed into a 20 mm × 20 mm square shape (about 0.4 mm thickness) and dried in a vacuum oven at 60 °C overnight to obtain its dry weight, represented by m_0 . Next,

the film was immersed in deionized water at 25 °C for 24 h to obtain its wet weight, denoted as m_1 . Notably, excess water on the surface of the samples was removed by filter paper. The formula for calculating water absorption was expressed as follows: $\omega = (m_1 - m_0) / m_0$. The melting temperature (T_m) was determined using a differential scanning calorimeter analyzer (DSC 200PC, manufactured by Netzsch in Germany). First, samples (3~5 mg) were heated to eliminate their thermal history. Next, the temperature was then reduced to -30 °C and heated to 120 °C at a rate of 10 °C min⁻¹. An empty aluminum crucible was utilized as the reference standard for all samples. The thermogravimetric analysis (TGA) of samples was measured using a TG-209F3 thermal analyzer (Netzsch, Germany). The sample (~5 mg) was heated from 45 °C to 690 °C at a heating rate of 10 °C min⁻¹. The tensile strength of the BWPU films was determined using an Electronic UTM6203 instrument (China). The film was cut into a 60 mm × 5 mm rectangular shape (approximately 0.4 mm thickness) for testing. Each film was measured three times in parallel. Dynamic mechanical analysis (DMA) curves were recorded on a dynamic mechanical analyzer (DMA-Q850, TA instruments, USA). Static contact angles of samples were determined using a contact angle goniometer (OCAH200, Dataphysics, Germany) at room temperature using the sessile drop method. The photochemical reactor was purchased from Chuanyi Experiment Instrument Co., Ltd (GY-GHX-DC, Shanghai, China).

4. Synthesis of Biomass-based Dienes and Diols.

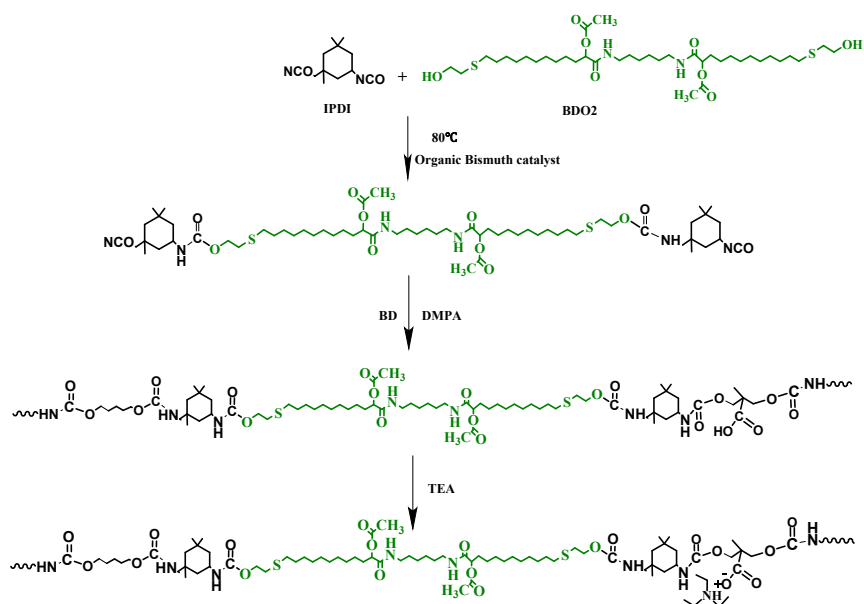
4.1 Synthesis of Biomass-based Dienes (BDEs). The BDEs were synthesized through the Passerini reaction using DICH, UA, and the specific acid component (C2, C4, C6, C8, or C10). Briefly, a single-mouth flask containing 24.2 mmol of UA (4.072 g), 24.2 mmol of acetic acid (1.452 g), and 12.1 mmol of DICH (1.648 g) in 40 mL of solvent (listed in **Table 1**) was stirred at room temperature (r.t.) or 35 °C for 24 h. The formation of the targeted product was monitored by TLC (hexane/ethyl acetate 5:1) analysis and the crude product was obtained *via* vacuum distillation. The resulting residue was further purified using column chromatography, yielding BDE as a light-yellow liquid or solid.

4.2 Synthesis of Biomass-based Diols (BDOs). BDOs were synthesized *via* a thiol-ene click reaction using BDEs and MO as raw materials. First, a solution of BDE2 (5.03 g, 8.5 mmol) and MO (1.32 g, 17 mmol) in ethanol (10 mL) was added to a 100 mL quartz tube. Second, the photoinitiator HM (0.127 g) was added to the mixture. Then the reaction was allowed to proceed for 3 h under irradiation from a 1000 W mercury lamp, with a circulating water system between the quartz tube and the lamp

to absorb the heat generated. Finally, the crude product was washed three times with water to remove MO, and then dehydrated by distillation under reduced pressure, yielding BDO as a light-yellow solid, 6.29g, yield of 99%.

5. Preparation of BWPU films.

The synthetic route and raw materials used for BWPU are shown in **Scheme S1** and **Table S2**, respectively. The R value was fixed at 1.2, and the hydrophilic chain extender DMPA content was maintained at 7%. Initially, BDOs, IPDI, and an organic bismuth catalyst (0.1 wt% of prepolymer's mass) were added into a three-necked flask equipped with an agitator and a thermometer and allowed to react at 85 °C for 2 h. Subsequently, 1,3-butanediol (BD) was added as the chain extender for 1 h. After the reaction mixture was cooled down to 50 °C, a DMF solution containing TEA and DMPA was added and stirred for an additional 4 h. Finally, BWPU emulsions with roughly 16 wt% solid content were obtained by emulsifying for 30 min with 50–60 g of deionized water under vigorous stirring. BWPU films can be prepared by drying at r.t. and further drying overnight at 60 °C in a vacuum drying oven.



Scheme S1. The synthetic route of BWPU.

Table S1. Sample designation and composition of BWPU emulsions.

Sample	BDOs, g	IPDI, g	BD, g	DMPA, g	R value ^a	DMPA ^b , %
BWPU2	5	4.3	0.36	0.730	1.2	7
BWPU4	5	4.2	0.37	0.720	1.2	7
BWPU6	5	4.1	0.38	0.715	1.2	7
BWPU8	5	4.0	0.38	0.710	1.2	7
BWPU10	5	3.9	0.38	0.700	1.2	7

^a R value (Isocyanate Index) = Molar ratio of -NCO/-OH. ^b Hydrophilic group content: DMPA% = Mass (DMPA) / Mass (BDOs + IPDI + BD + DMPA) × 100%.

Table S2. Physicochemical parameters of BDOs.

Sample	Physical form (r.t.)	Melting point (°C)	Hydroxyl value (mg KOH/g)
BDO2	solid	46.3	150 ± 2.0
BDO4	solid	55.9	139 ± 2.0
BDO6	solid	47.8	130 ± 2.0
BDO8	solid	37.9	122 ± 2.0
BDO10	solid	48.2	115 ± 2.0

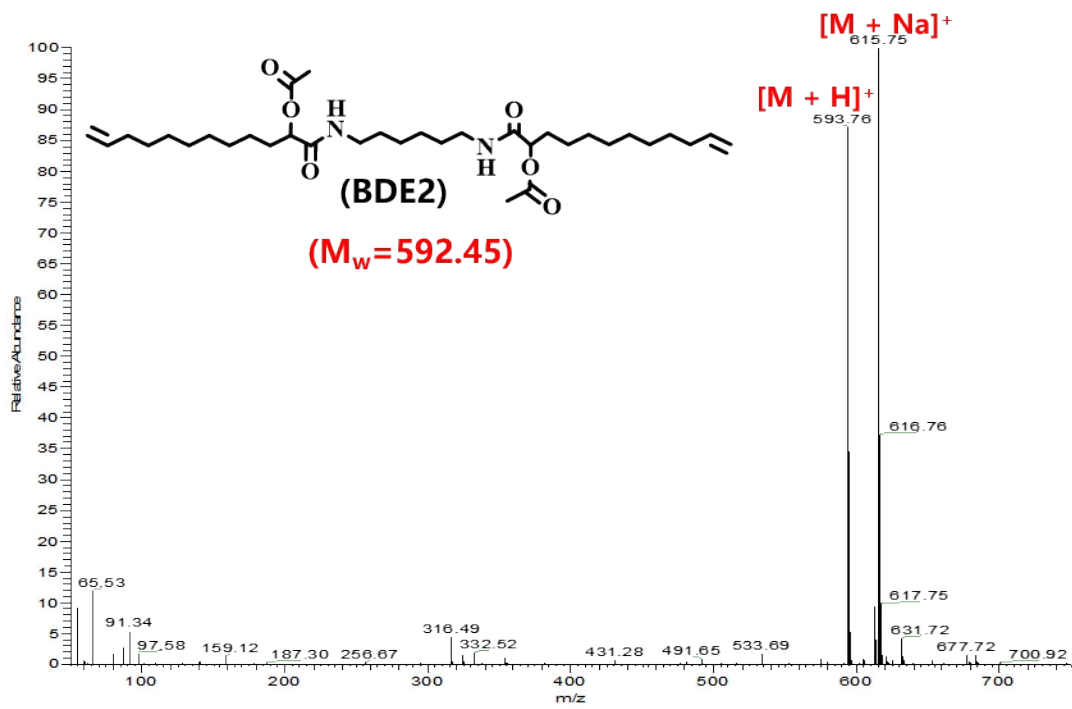


Figure S1. The mass spectrum of BDE2 (C₃₄H₆₀N₂O₆).

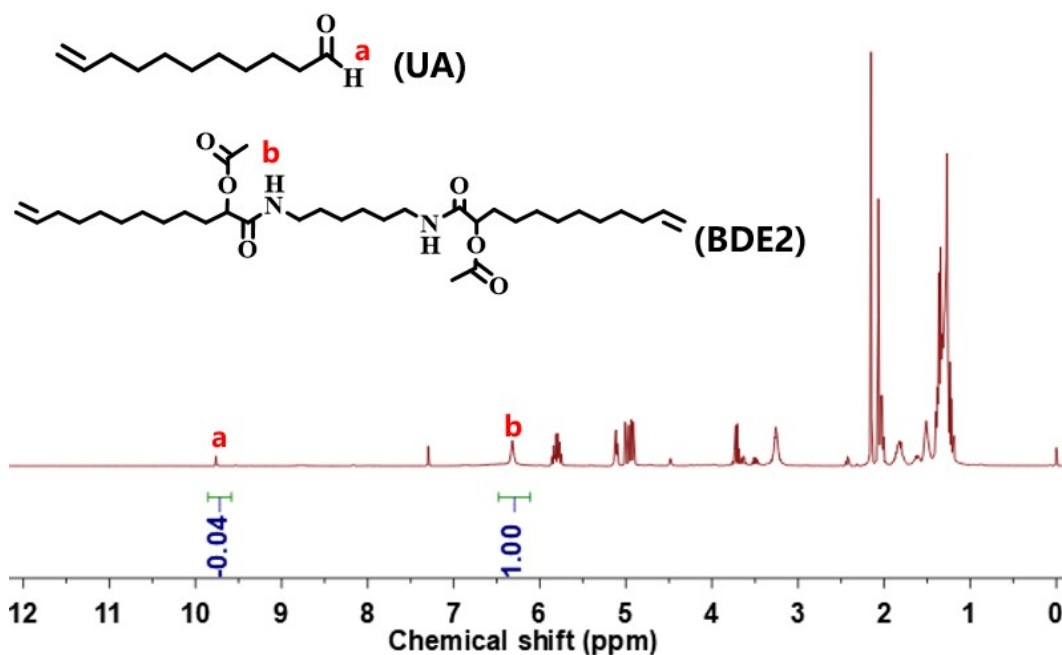


Figure S2. The ^1H NMR (25 °C, 400 MHz) spectrum of the crude product in CDCl_3 . As the Passerini reaction progresses, although the integrated area at point a in the crude product will gradually decrease (indicating the consumption of UA), the sum of the integrated areas at points a and b remains constant. Therefore, by dividing the integrated area at point b by the total integrated area at points a and b in the crude product, the yield of BDE2 can be calculated. Based on our calculations under the employed reaction conditions, the yield of BDE2 in ethanol at 40 °C was determined to be 96.2%.

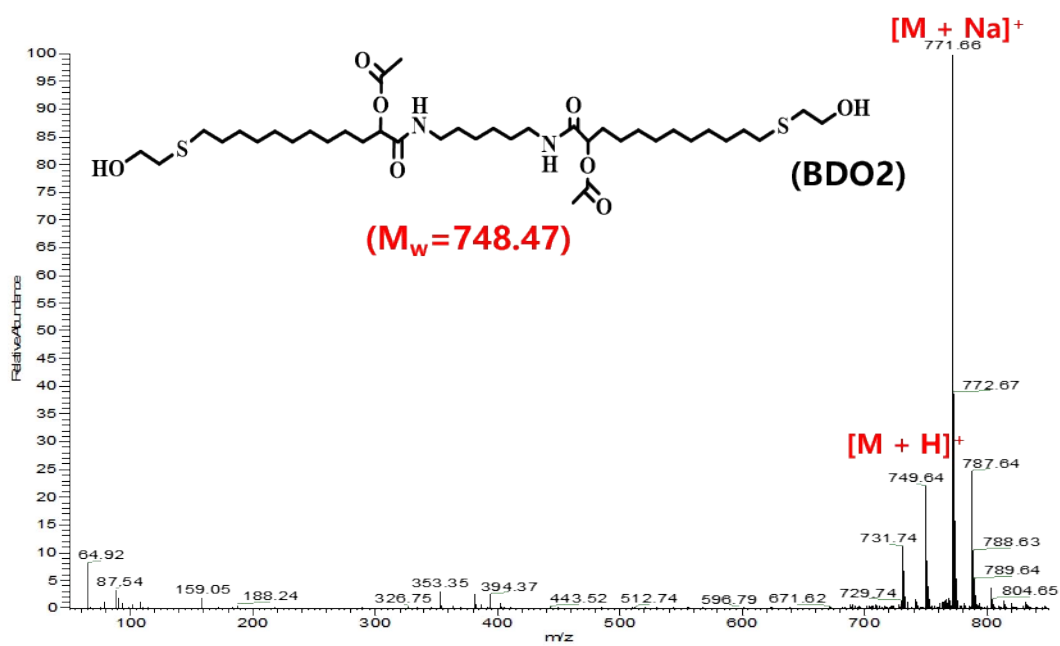


Figure S3. The mass spectrum of BDO2 (C₃₈H₇₂N₂O₈S₂).

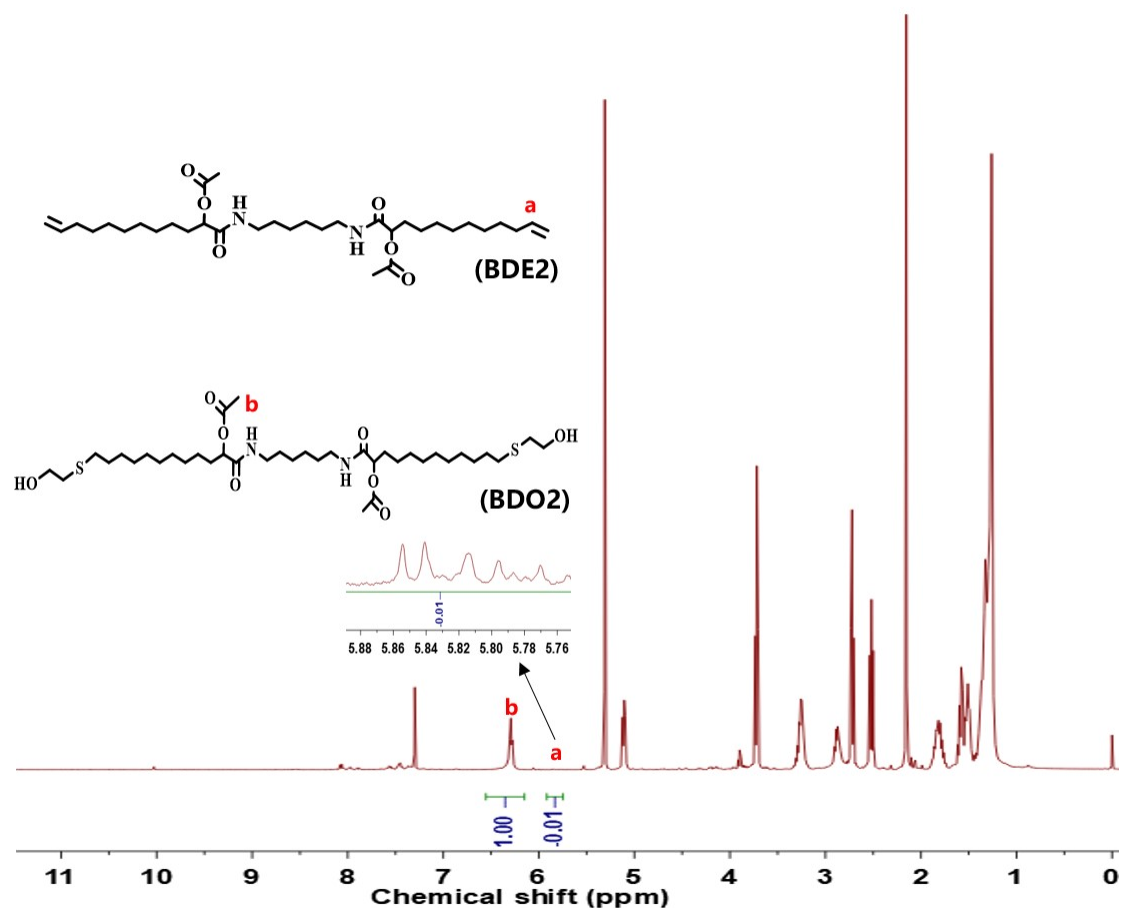


Figure S4. The ¹H NMR (25 °C, 400 MHz) spectrum of the crude product in CDCl₃. As the click reaction undergoes, the integrated area of BDE2 at the peak **a** will gradually decrease, while the integrated area at peak **b** (hydrogen in the amide group) remains unchanged. Therefore, by utilizing the ratio of these two integrated areas in the crude product, it is possible to calculate the conversion rate of BDE2 or the yield of BDO2. Based on our calculations under the employed reaction conditions, the yield of BDO2 was determined to be 99%.

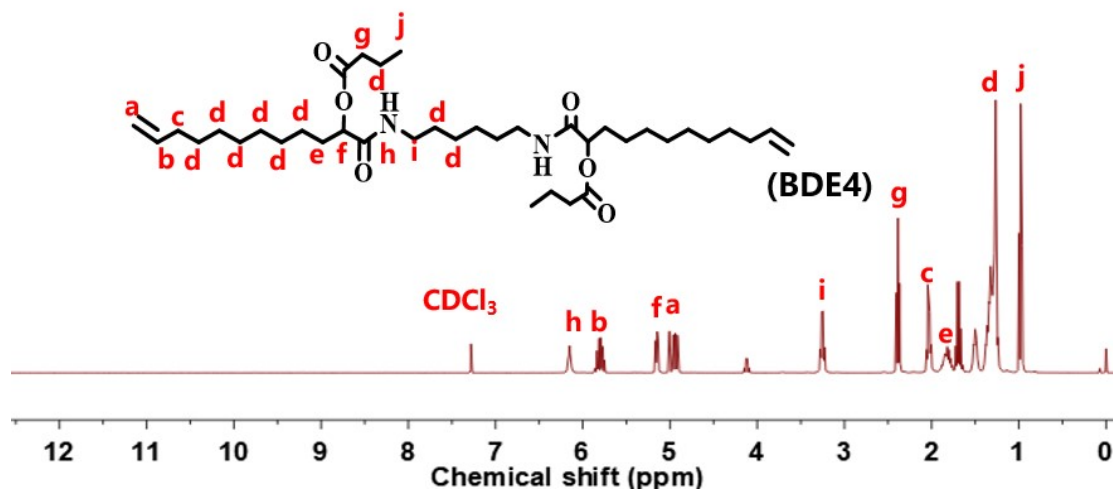


Figure S5. The ^1H NMR (25 °C, 400 MHz) spectrum of BDE4 in CDCl_3 .

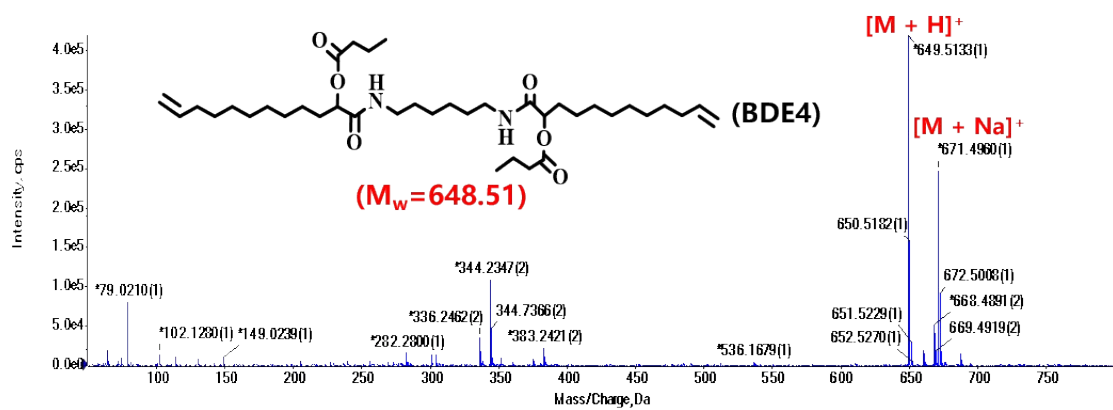


Figure S6. The mass spectrum of BDE4 ($\text{C}_{38}\text{H}_{68}\text{N}_2\text{O}_6$).

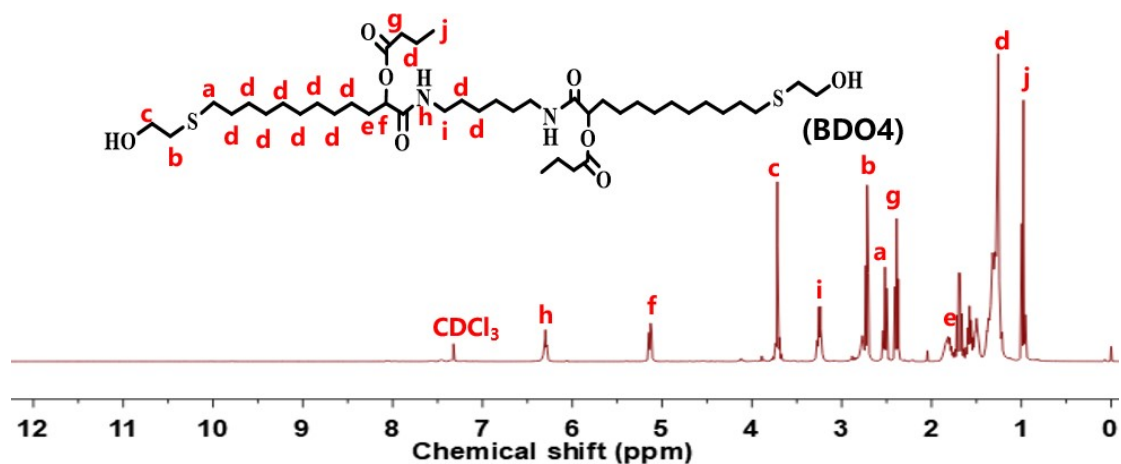


Figure S7. The ¹H NMR (25 °C, 400 MHz) spectrum of BDO4 in CDCl₃.

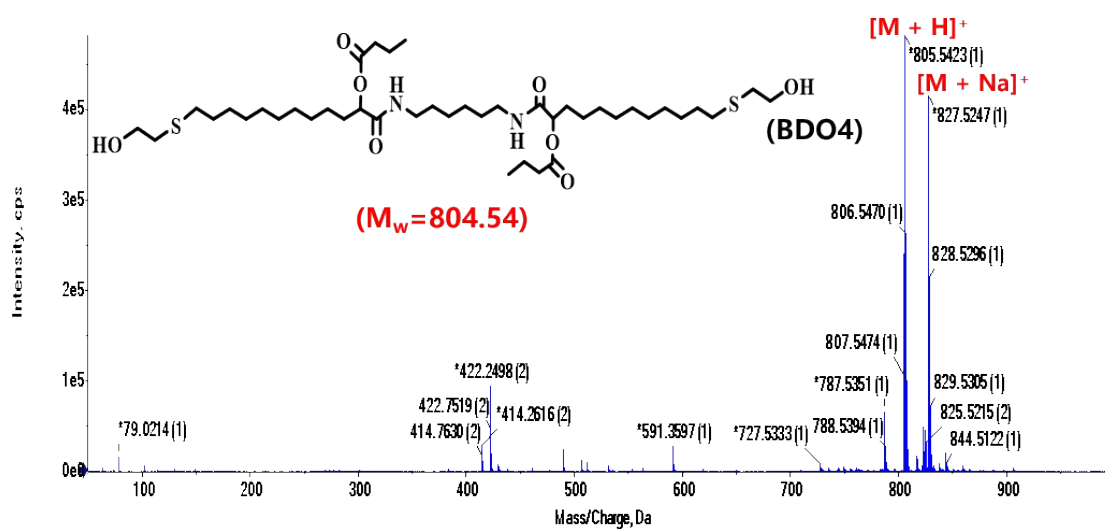


Figure S8. The mass spectrum of BDO4 (C₄₂H₈₀N₂O₈S₂).

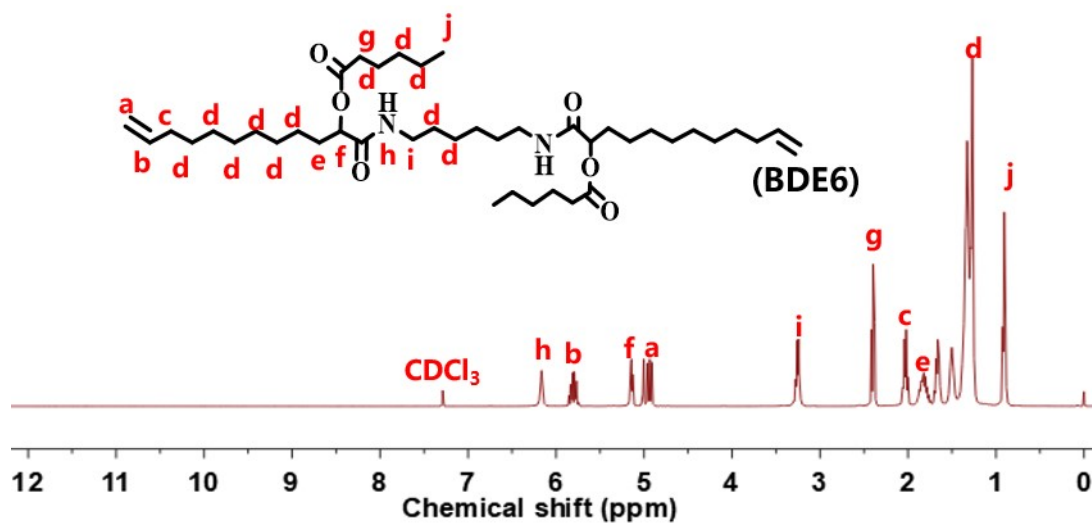


Figure S9. The ¹H NMR (25 °C, 400 MHz) spectrum of BDE6 in CDCl₃.

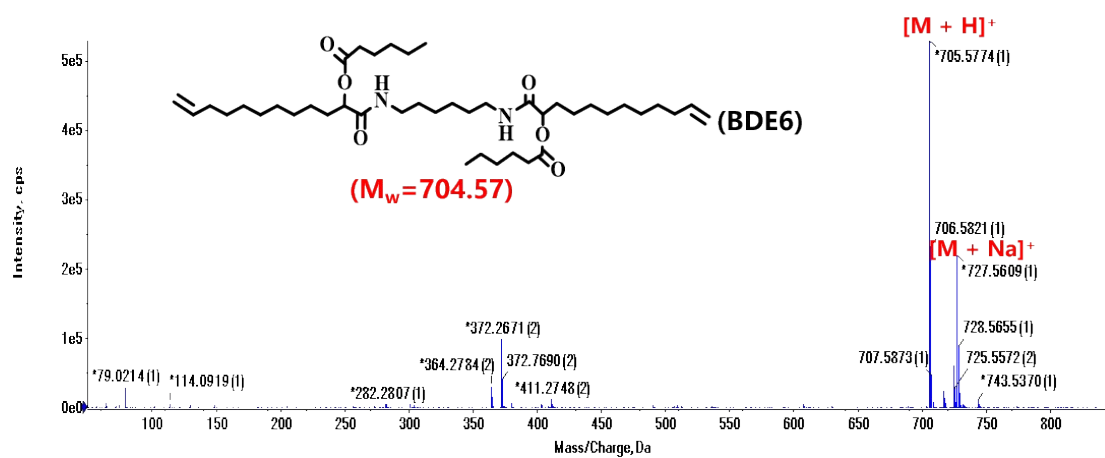


Figure S10. The mass spectrum of BDE6 (C₄₂H₇₆N₂O₆).

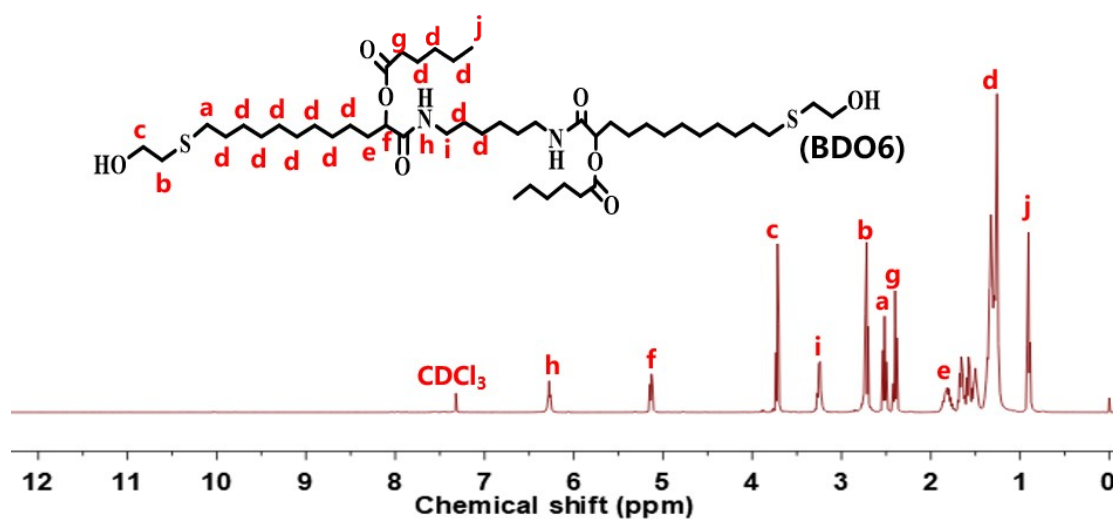


Figure S11. The $^1\text{H NMR}$ (25 °C, 400 MHz) spectrum of BDO6 in CDCl_3 .

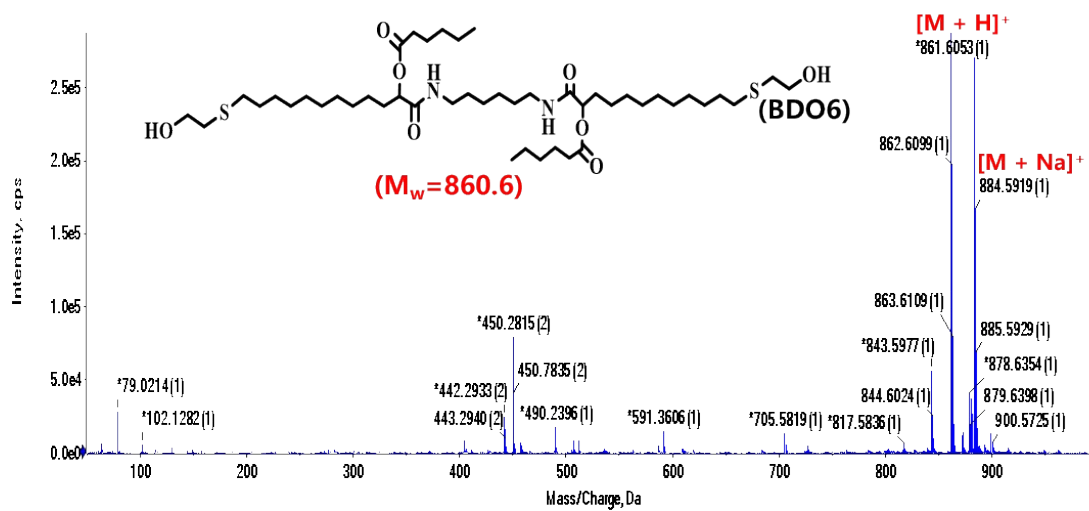


Figure S12. The mass spectrum of BDO6 ($\text{C}_{46}\text{H}_{88}\text{N}_2\text{O}_8\text{S}_2$).

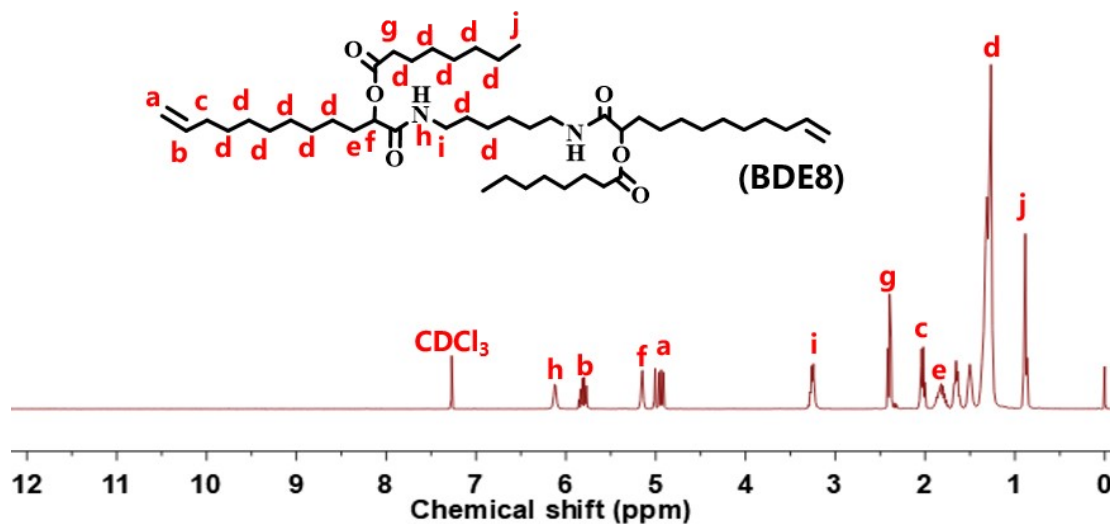


Figure S13. The ^1H NMR (25 °C, 400 MHz) spectrum of BDE8 in CDCl_3 .

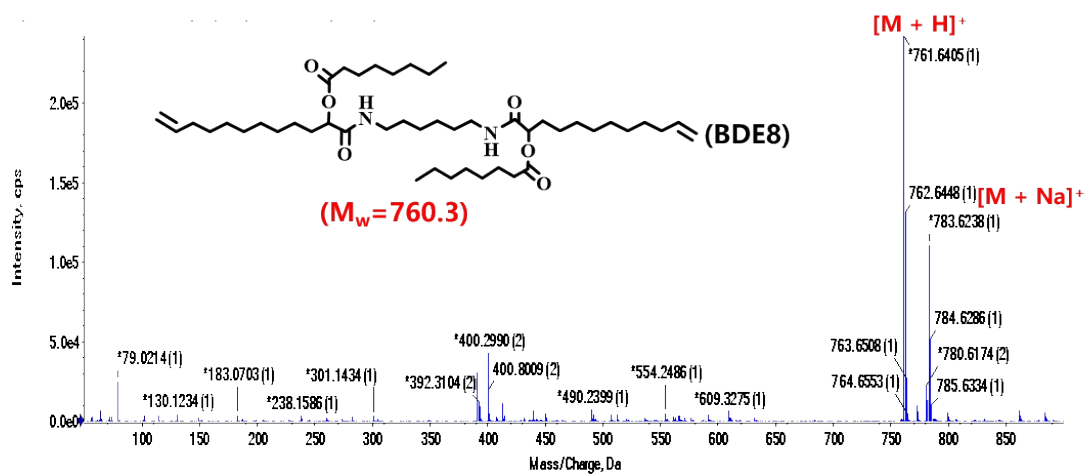


Figure S14. The mass spectrum of BDE8 ($\text{C}_{46}\text{H}_{84}\text{N}_2\text{O}_6$).

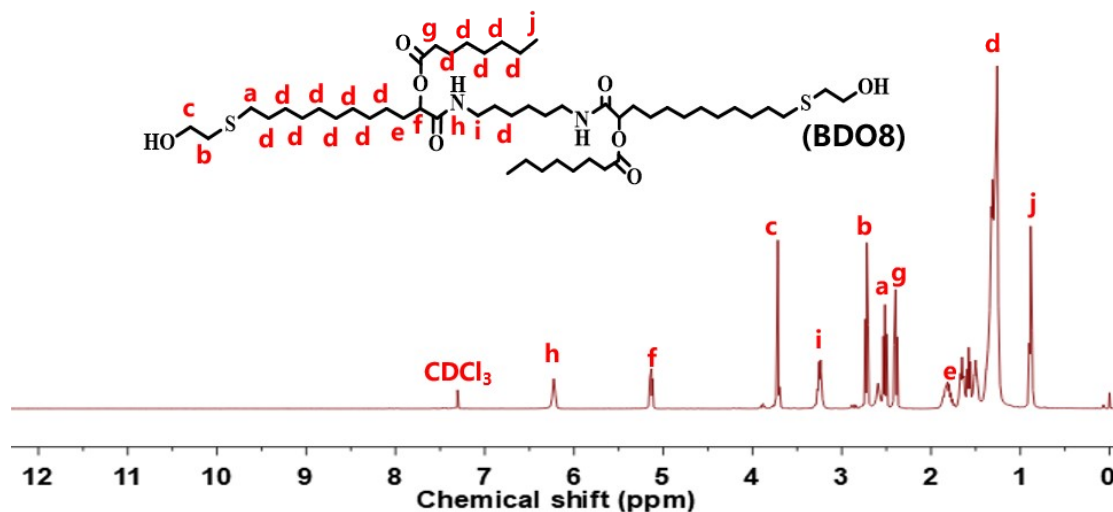


Figure S15. The ¹H NMR (25 °C, 400 MHz) spectrum of BDO8 in CDCl₃.

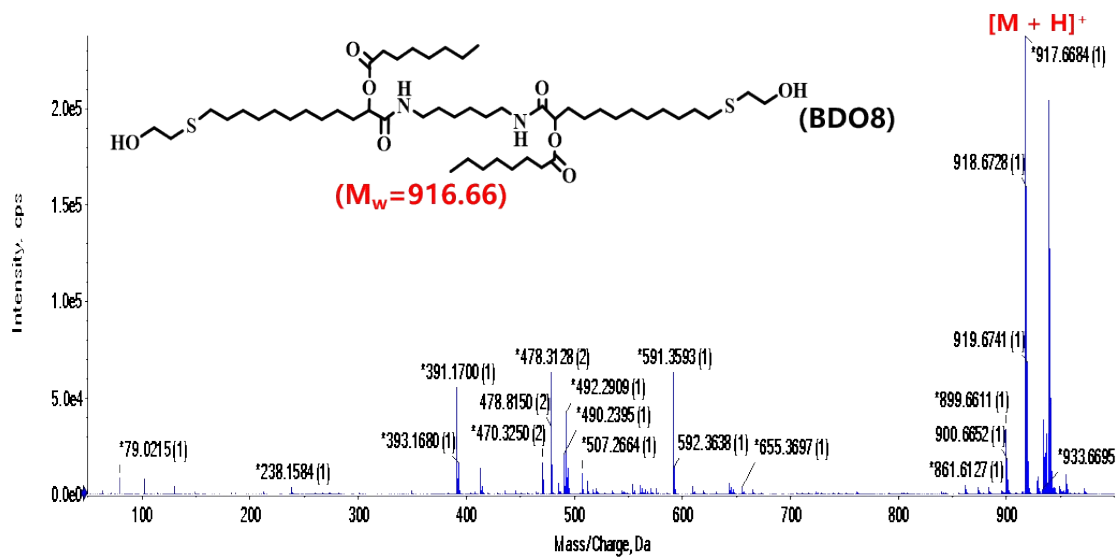


Figure S16. The mass spectrum of BDO8 (C₅₀H₉₆N₂O₈S₂).

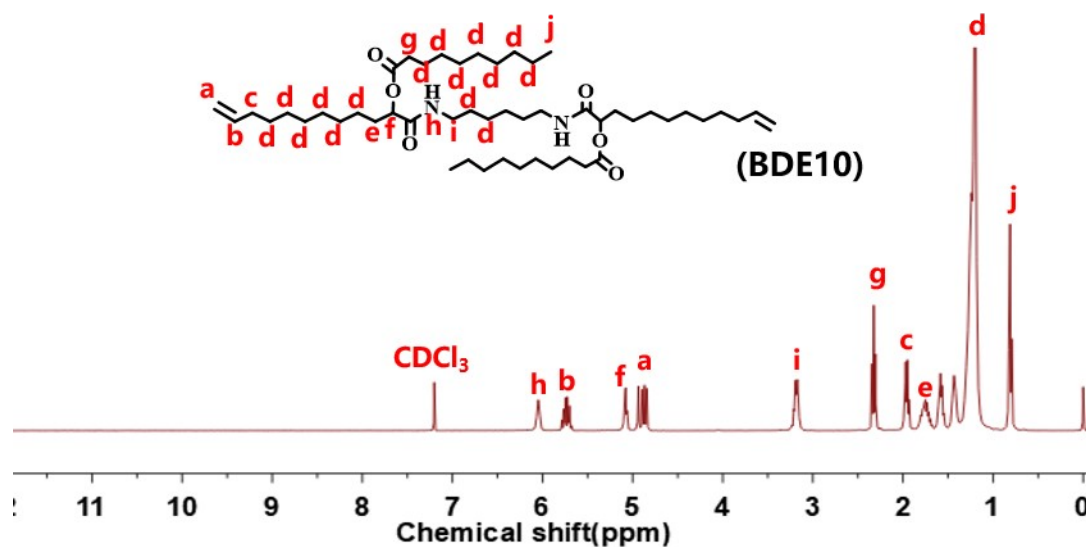


Figure S17. The ¹H NMR (25 °C, 400 MHz) spectrum of BDE10 in CDCl₃.

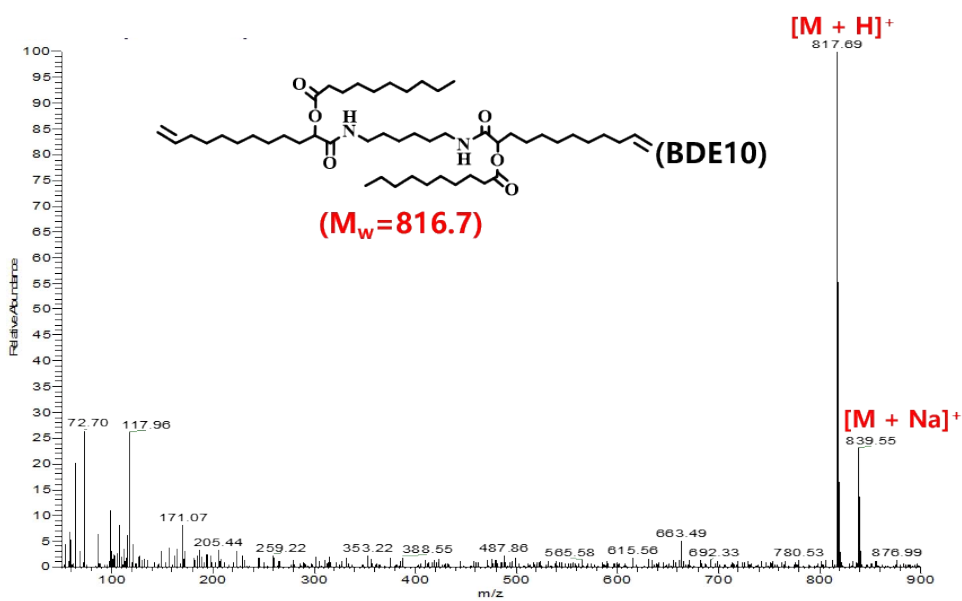


Figure S18. The mass spectrum of BDE10 (C₅₀H₉₂N₂O₆).

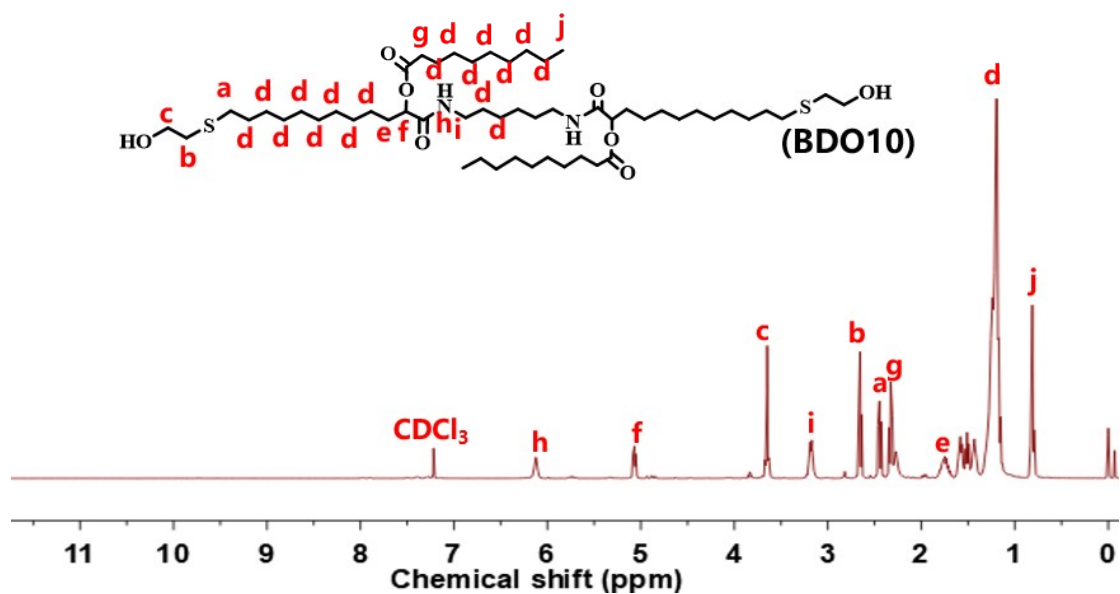


Figure S19. The ^1H NMR (25 °C, 400 MHz) spectrum of BDO10 in CDCl_3 .

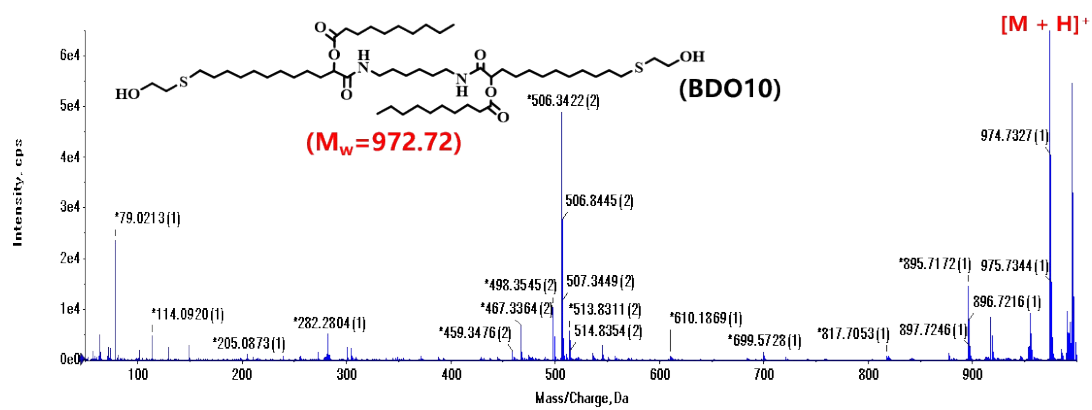


Figure S20. The mass spectrum of BDO10 ($\text{C}_{54}\text{H}_{104}\text{N}_2\text{O}_8\text{S}_2$).

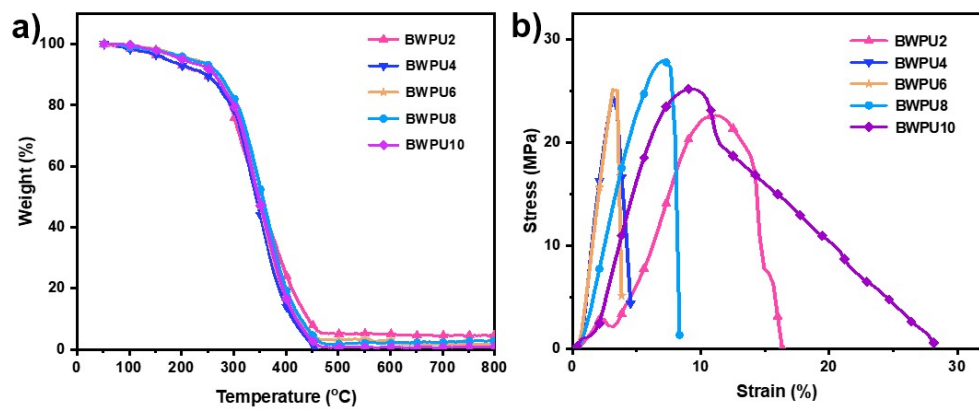


Figure S21. (a) TGA curves. (b) Stress-strain curves.

Reference

1. Kreye O, Tóth T, Meier MAR. Introducing Multicomponent Reactions to Polymer Science: Passerini Reactions of Renewable Monomers. **Journal of the American Chemical Society** **2011**, 133(6): 1790-1792.
2. Mutlu H, Meier MAR. Castor oil as a renewable resource for the chemical industry. **European Journal of Lipid Science and Technology** **2010**, 112(1): 10-30.
3. Sehlinger A, Dannecker P-K, Kreye O, Meier MAR. Diversely Substituted Polyamides: Macromolecular Design Using the Ugi Four-Component Reaction. **Macromolecules** **2014**, 47(9): 2774-2783.
4. Khamphajun K, Namnouad P, Docker A, Ruengsuk A, Tantirungrotechai J, Díaz-Torres R, *et al.* Neutral isocyanide-templated assembly of pillar[5]arene [2] and [3]pseudorotaxanes. **Chemical Communications** **2022**, 58(52): 7253-7256.
5. Mi J, Liu S, Qi H, Huang J, Lan X, Zhang L. Cellular Engineering and Biocatalysis Strategies toward Sustainable Cadaverine Production: State of the Art and Perspectives. **ACS Sustainable Chemistry & Engineering** **2021**, 9(3): 1061-1072.
6. Chae TU, Ahn JH, Ko Y-S, Kim JW, Lee JA, Lee EH, *et al.* Metabolic engineering for the production of dicarboxylic acids and diamines. **Metabolic Engineering** **2020**, 58: 2-16.
7. Wang L, Li G, Deng Y. Diamine Biosynthesis: Research Progress and Application Prospects. **Applied and Environmental Microbiology** **2020**, 86(23): e01972-01920.
8. Sarchami T, Batta N, Berruti F. Production and separation of acetic acid from pyrolysis oil of lignocellulosic biomass: a review. **Biofuels, Bioproducts and Biorefining** **2021**, 15(6): 1912-1937.
9. Salvachúa D, Saboe PO, Nelson RS, Singer C, McNamara I, del Cerro C, *et al.* Process intensification for the biological production of the fuel precursor butyric acid from biomass. **Cell Reports Physical Science** **2021**, 2(10): 100587.
10. Chen W-S, Strik DPBTB, Buisman CJN, Kroeze C. Production of Caproic Acid from Mixed Organic Waste: An Environmental Life Cycle Perspective. **Environmental Science & Technology** **2017**, 51(12): 7159-7168.
11. Hidajat MJ, Kwon O, Park H, Han J, Yun G-N, Hwang DW. Highly selective, energy-free, and environmentally friendly one-pot production of linear α -olefin from biomass-derived organic acid in a dual-bed catalyst system. **Green Chemistry** **2022**, 24(19): 7556-7573.
12. Kim S, Gonzalez R. Selective production of decanoic acid from iterative reversal of β -oxidation pathway. **Biotechnology and Bioengineering** **2018**, 115(5): 1311-1320.
13. Faveere WH, Van Praet S, Vermeeren B, Dumoleijn KNR, Moonen K, Taarning E, *et al.* Toward Replacing Ethylene Oxide in a Sustainable World: Glycolaldehyde as a Bio-Based C2 Platform Molecule. **Angewandte Chemie International Edition** **2021**, 60(22): 12204-12223.